Impact of Tropical Indian Ocean Temperature on the Ozone Layer in East Asia

Mengkun TIAN[1], Yiran GUO[1], Xiuying WANG[2], Yan CHEN[3], Shichang GUO[1]*

1. Department of Atmosphere Science, Yunnan University, Kunming 650091, China; 2. Pu'er Meteorological Bureau, Pu'er 665000, China; 3. Yunnan Weather Bureau, Kunming 650034, China

Abstract Based on the reanalysis data of monthly mean sea surface temperature (SST) from British Hadley Center and ozone mass mixing ratio from National Aeronautics and Space Administration (NASA) during 1980-2015, two indexes IOBI and IODI of the main modes characterizing SST changes in the tropical Indian Ocean——Indian Ocean Basin (IOB) and Indian Ocean Dipole (IOD) were calculated firstly, and then the correlation of SST anomaly (SSTA) in the tropical Indian Ocean and ozone mass mixing ratio in the stratosphere over East Asia from 1980 to 2015 was analyzed. Besides, the impact of SST changes in the tropical Indian Ocean on the distribution of ozone layer in East Asia was discussed. The results show that SST changes in the tropical Indian Ocean had significant effects on stratospheric ozone distribution in East Asia, and it was consistent with the temporal changes of IOB and IOD. IOBI and IODI had a certain correlation with stratospheric ozone changes in East Asia, with a particularly significant correlation in the lower stratosphere (70 hPa) and middle stratosphere (40 hPa) especially during spring and autumn.

Key words Tropical Indian Ocean; East Asia; Indian Ocean Basin; Indian Ocean Dipole; Stratospheric ozone

DOI 10.19547/j.issn2152-3940.2023.06.001

Angione *et al.* [1] measured ozone as one of important atmospheric components. By observations, it is found that ozone is mainly concentrated in the upper air at 10-50 km[2], and ozone content is high in the air above 20 km, which is called the atmospheric ozone layer[3]. Ozone can reflect the change of atmospheric circulation, and too high ozone concentration will also cause climate and environmental changes. As a protective layer, ozone in the stratosphere can reduce the short-wave radiation reaching the ground. In the troposphere, ozone absorbs long-wave radiation from the ground to heat the atmosphere. The high concentration of ozone near the ground will cause bronchi, skin cancer and other diseases[4]. Therefore, the changing characteristics of ozone have become one of research objects that domestic and foreign scholars pay attention to[5-6]. In East Asia as a concentrated area of the global population, human activities will also be affected and restricted by the changes in the upper atmospheric environment and ozone concentration[7]. Therefore, it is of great scientific significance to study the factors causing the anomaly and change of ozone layer distribution in East Asia.

There are many factors affecting the change of ozone content, such as the circulation change process of planetary wave propagation and Hadley circulation activity[8-12]. Some studies have shown that changes in ozone also contain fluctuation signals sea surface temperature (SST)[13-14]. With the in-depth understanding of SST changes, the impact of SST changes on the spatial distribution of ozone has been gradually paid attention to and studied by scholars[15]. The Indian Ocean has attracted much attention from scientists. Saji *et al.* [16-17] found that there are two main distribution modes of SST anomalies in the tropical Indian Ocean, of which the first main mode is Indian Ocean Basin (IOB) with consistent warming or cooling of SST in the tropical Indian Ocean, and the second main mode Indian Ocean Dipole (IOD) means that the SST anomalies in the southeast and northwest tropical Indian Ocean were reverse seesaw dipoles. The impact of the main modes in the tropical Indian Ocean on ozone has also attracted the attention of scholars. Nassar *et al.* [18] proposed that the sharp decline in ozone content over the western Indian Ocean and Africa in 2006 may be caused by strong local convection resulting from IOD. Takashi *et al.* [19] studied the factors affecting the annual variation of tropospheric ozone in the northern Hemisphere, and found that the change of SST in the Indian Ocean would affect the interannual signal of tropospheric ozone. Krzyscin *et al.* [20] analyzed the ozone change in the Northern Hemisphere. It is found that independent positive IOD events in spring would change the total ozone content in areas near the equator; independent positive IOD events in autumn increased total ozone content at 30°-35° N and decreased total ozone content at 65°-70° N.

Although the impact of SST changes in the Indian Ocean on ozone distribution in some regions has been discussed in the past, there are relatively few studies on the relationship between stratospheric ozone concentration changes in East Asia and SST anomaly (SSTA) in the tropical Indian Ocean. In this paper, based on more complete and continuous data of SST and reanalysis data of ozone mixing ratio, the relationship between the two main modes of SST changes in the tropical Indian Ocean and the ozone layer

Received: November 12, 2023 Accepted: December 16, 2023

Supported by the National Natural Science Foundation of China (41275072, 41365007); (Key) Project for Applied Basic Research of Yunnan Province (2011FA031).

* Corresponding author.

change in East Asia was studied.

1 Data and methods

The data of monthly mean SST from the HadISST dataset of Hadley Center of the UK Met Office as well as the data of monthly mean ozone mixing ratio from the MERRA data of the National Aeronautics and Space Administration (NASA) were used in this study. The research methods used include EOF analysis, correlation analysis, and SVD decomposition. Ozone is mainly concentrated in the stratosphere, so the ozone mixing ratio of the stratosphere in East Asia was selected for related research. The study period is from 1980 to 2015, 36 years in total. The study areas are the tropical Indian Ocean (25° S – 25° N, 40° E – 120° E) and East Asia (2° N – 56° N, 72° E – 136° E).

2 Calculation of the main mode indices of SST changes in the tropical Indian Ocean and their correlation with the ozone mixing ratio over the East Asia

2.1 Calculation of IOBI and IODI According to the study area and the previous definition of IOB, SSTA in the tropical Indian Ocean (25° S – 25° N, 40° E – 120° E) in spring was selected for EOF analysis, and the spatial distribution of EOF1 was IOB. After deducting the linear trend and standardizing its time series (PC1), the IOB index (IOBI) representing the feature changes of IOB was calculated, and its time series is shown in Fig. 1.

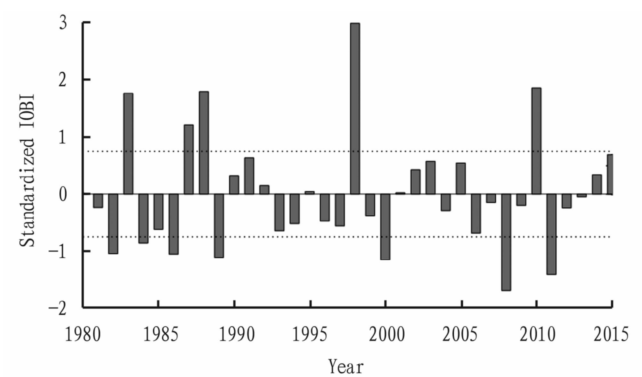

Note: Dotted lines mean the standard deviations of IOBI with the absolute value great than 0.75.

Fig. 1 Standardized IOBI during 1980 – 2015

According to the Indian Ocean Dipole Index (IODI) defined by Saji *et al.* [16], the time series of IODI was calculated based on the difference between the regional mean SSTA of the northwestern (10° S – 10° N, 50° E – 70° E) and southeastern (10° S – EQ, 90° E – 110° E) tropical Indian Ocean in autumn (Fig. 2). The correlation coefficient of IODI and EOF2 time series of SSTA in the tropical Indian Ocean in autumn was 0.69, passing 99% significance t test, so the time series of IODI calculated can be trusted, and can be used to characterize the changes of SSTA in the east and west of the tropical Indian Ocean.

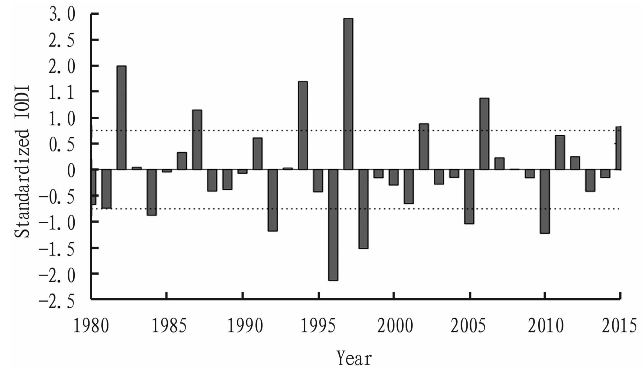

Note: Dotted lines mean the standard deviations of IODI with the absolute value great than 0.75.

Fig. 2 Standardized IODI during 1980 – 2015

2.2 Analysis of the correlation between IOBI or IODI and ozone mixing ratio in East Asia Before the correlation analysis, seasonal zonal averaging of the ozone mixing ratio data in East Asia was conducted and processed into height – latitude data at 2° N – 56° N. Then, the correlation coefficients of IOBI and IODI with the ozone layer in East Asia were calculated to obtain the vertical distribution of the correlation coefficients (Fig. 3 and Fig. 4). In the figures, the contour lines represent correlation coefficient values, of which the solid line represents the positive value, and the dashed line represents the negative value. The interval of the contour lines is 0.05, and the color part means passing the 90% confidence t test.

Fig. 3 shows the seasonal correlation between IOBI and stratospheric ozone mixing ratio in East Asia during 1980 – 2015. As can be seen from the figure, there were significant differences in the correlation between IOBI and stratospheric ozone in different seasons. With the change of seasons, the correlation areas and intensity between the two also changed.

From the perspective of latitude distribution, the evolution process of the correlation between IOBI and ozone can be divided into two parts: there was a negative correlation in the low-latitude region (south of 25° N) and a positive correlation in the middle-latitude region (north of 25° N) in East Asia, and the correlation distribution moved from north to south with the change of seasons. In winter, the effect of IOB on ozone content in East Asia mainly appeared at 20 – 30 and 70 hPa in the stratosphere in the low latitudes, and the correlation was mainly negative. In spring and summer, the correlation was negative in the lower and middle stratosphere in the low latitudes and positive in the lower stratosphere in the middle latitudes, and both positive and negative correlation were stronger. In autumn, there was a significant negative correlation in the middle stratosphere. The significant area gradually weakened and moved to the north, possibly because IOB was weaker in autumn.

When the variation of SST in tropical Indian Ocean was shown as IOB, the SSTA in the tropical Indian Ocean would affect the distribution of stratospheric ozone in East Asia. When IOB was positive, the SST in the tropical Indian Ocean was uniformly higher, and ozone content was higher in the positive correlation region and lower in the negative correlation region in East Asia. It was opposite as IOB was negative. This impact was different in different latitudes and altitudes, which was most obvious in spring. When IOB weakened gradually, the impact of SSTA on ozone distribution also decreased gradually.

Seen from Fig. 4, the correlation between IODI and stratospheric ozone in East Asia was also spatially different. With the change of seasons, the correlation area and intensity between the two also changed.

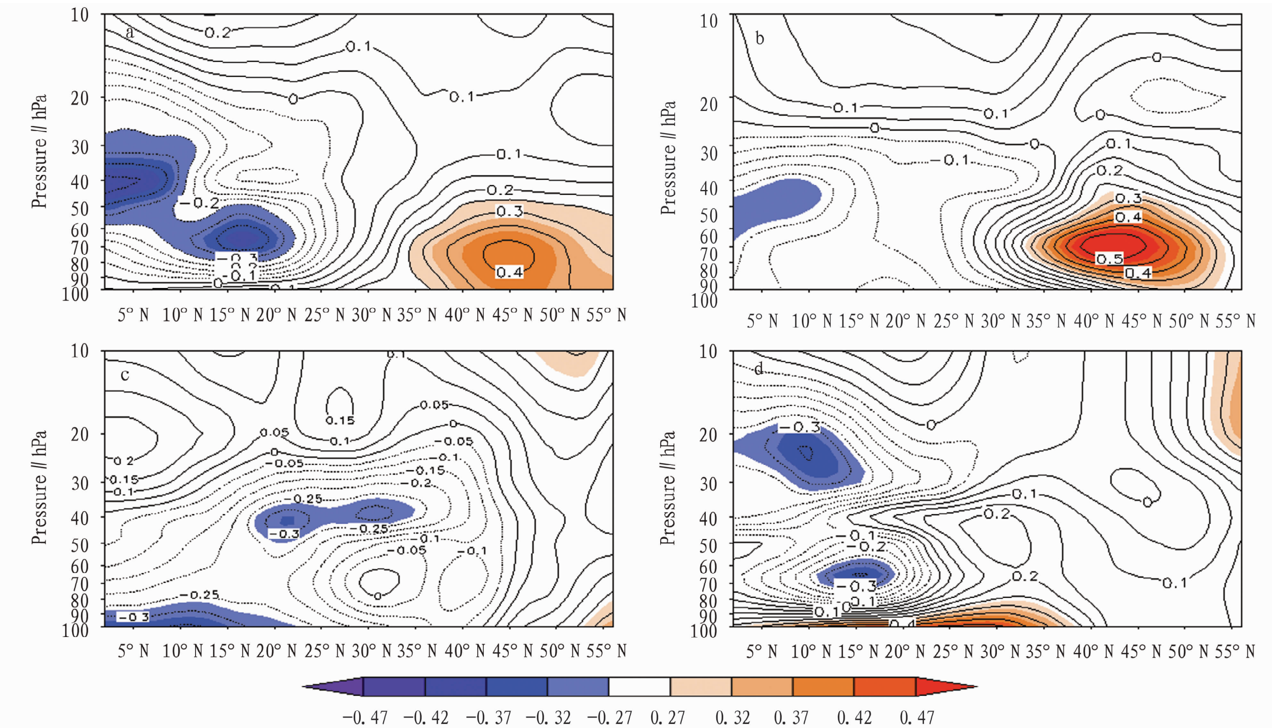

Note: a. Spring; b. Summer; c. Autumn; d. Winter.

Fig. 3 Vertical distribution of the correlation coefficient of IOBI and ozone in East Asia

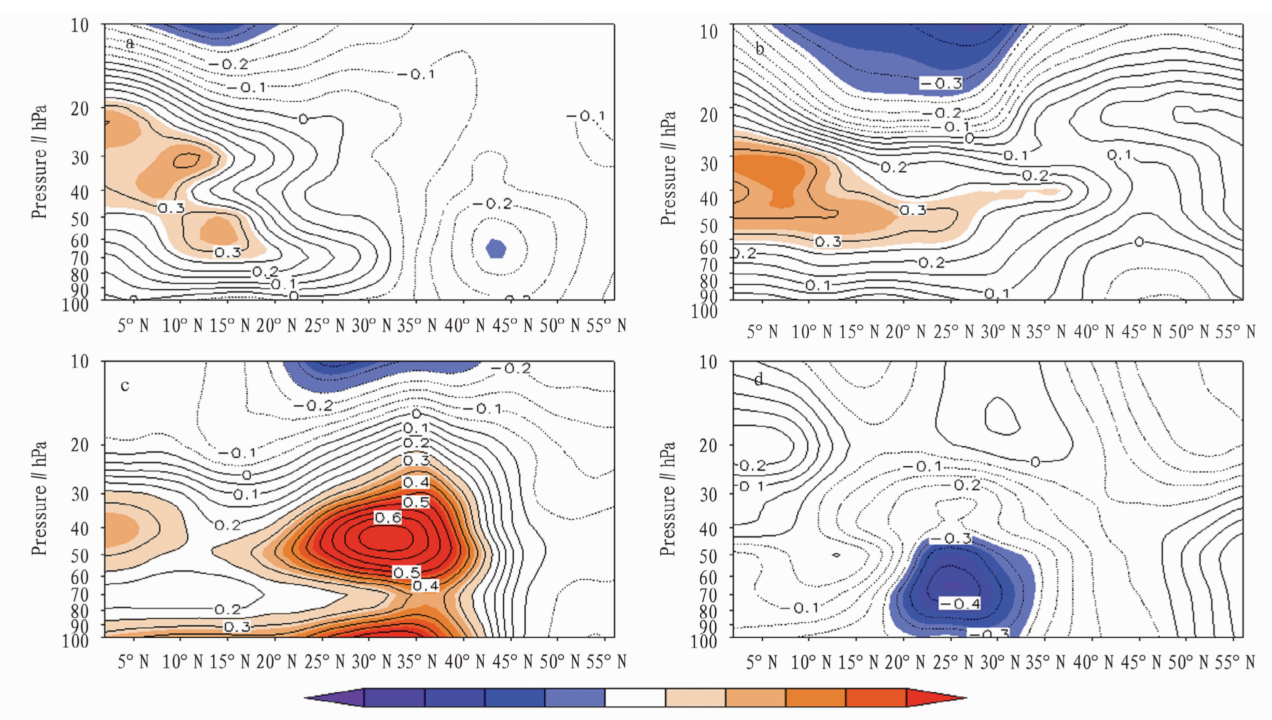

Note: a. Spring; b. Summer; c. Autumn; d. Winter.

Fig. 4 Vertical distribution of the correlation coefficient of IODI and ozone in East Asia

The evolution of the correlation between IODI and ozone mixing ratio in East Asia can be started in winter. In winter, the correlation was negative in the low and middle latitudes of East Asia, and the large-value area of significant correlation appeared at 20° N – 35° N, that is, there was a significant correlation from the lower stratosphere to the middle stratosphere. In spring, the negative correlation in the low latitudes of East Asia changed to positive correlation, and the negative correlation in the middle latitudes weakened and retreated to the north. In summer, the significant positive correlation area tended to expand northward, and gradually covered the middle stratosphere in the low and middle latitudes of East Asia. By autumn, the significant positive correlation area continued to expand and developed towards the upper stratosphere, even exceeding 30 hPa.

Based on the above analysis, when the variation of SST in the tropical Indian Ocean was shown as IOD, the SSTA in the tropical Indian Ocean would also affect the stratospheric ozone distribution in East Asia. When IOD was positive, the SST in the tropical Indian Ocean was high in the west and low in the east. The ozone content in the positively correlated area was higher than that in the negatively correlated area. It was opposite as IOD was negative. This impact seemed to be related to the intensity of IOD, and there was a seasonal change with the development of IOD. This impact was most pronounced in autumn when IOD matured, and the correlation gradually weakened after IOD weakened.

3 SVD decomposition of SST in the tropical Indian Ocean and stratospheric ozone mixing ratio in East Asia

3.1 Spring From the above analysis of the correlation, it can be found that the ozone at 40 and 70 hPa was significantly affected by SST changes in the tropical Indian Ocean. In spring and autumn, ozone content was significantly affected by SST changes, and IOB or IOD was strong. Therefore, the SST in the tropical Indian Ocean and the ozone mixing ratio at 40 and 70 hPa in spring and autumn were selected for SVD decomposition. In this section, the distribution of heterogeneous correlation coefficient of SVD modes and their corresponding time series were mainly analyzed, and the calculation results of the modes with cumulative square covariance contribution rate (CSCF) reaching 70% were selected for analysis.

3.1.1 70 hPa. The correlation coefficient of the first mode obtained by SVD between SST field in the tropical Indian Ocean and the ozone field at 70 hPa in the stratosphere in East Asia was 0.58, and the square covariance contribution rate (SCF) was 81.62%. Hence, the first mode of SVD decomposition can represent the main characteristics of the interaction between the SST field and the ozone field, as well as the teleconnection between the SST changes in the tropical Indian Ocean and the stratospheric ozone distribution at 70 hPa in East Asia in spring. As can be seen from Fig. 5, in the SST field in tropical Indian Ocean, SST in the whole region presented a consistent positive correlation, and the maximum was located in the Arabian Sea and Bay of Bengal waters to the east of Madagascar and north of the equator, indicating that the SSTA in the tropical Indian Ocean in spring can affect the distribution of stratospheric ozone layer at 70 hPa in East Asia during the same period. In the stratospheric ozone field at 70 hPa in East Asia, bounded by 30° N, the correlation coefficient was negative in south and positive in north. The large-value area of positive correlation was located in the central and western part of Mongolia, from the western part of Inner Mongolia to Xinjiang and Balkhash Lake. The large-value area of negative correlation appeared in the Indian Peninsula and the Bay of Bengal to the south of 25° N as well as the Indochina Peninsula and the South China Sea to the east. When the SST change in the tropical Indian Ocean was shown as positive IOB, the stratospheric ozone content in the low latitudes decreased but increased in the middle latitudes at 70 hPa in East Asia. As the SST change in the tropical Indian Ocean was shown as negative IOB, the ozone distribution in East Asia was reverse. The conclusions of SVD decomposition were basically consistent with the results of correlation analysis. From the time coefficient of the first mode (Fig. 6), it can be seen that the corresponding relationship between the two was good.

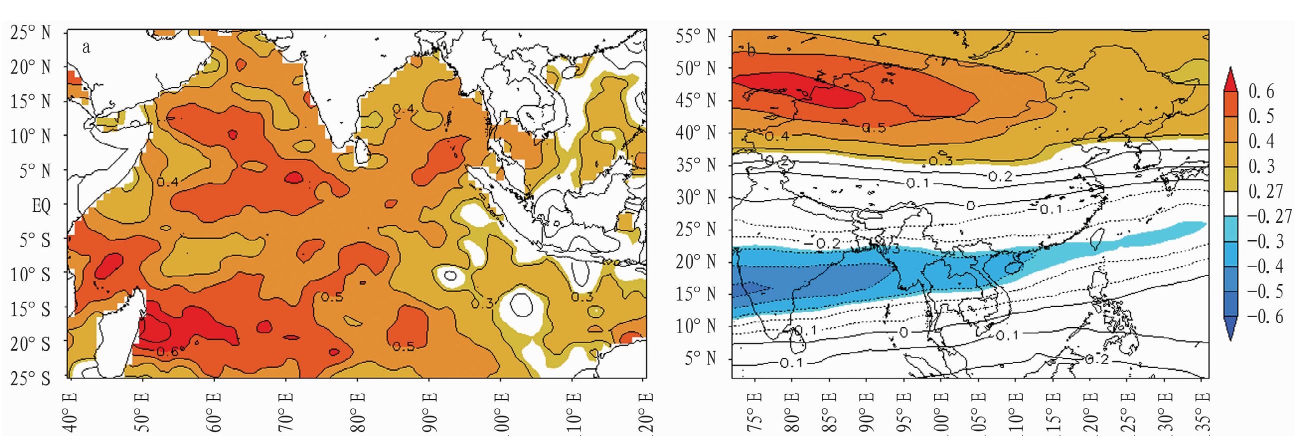

Fig. 5 Spatial distribution of the first mode obtained by SVD decomposition for the SST (a) in the tropical Indian Ocean and stratospheric ozone (b) at 70 hPa in East Asia in spring

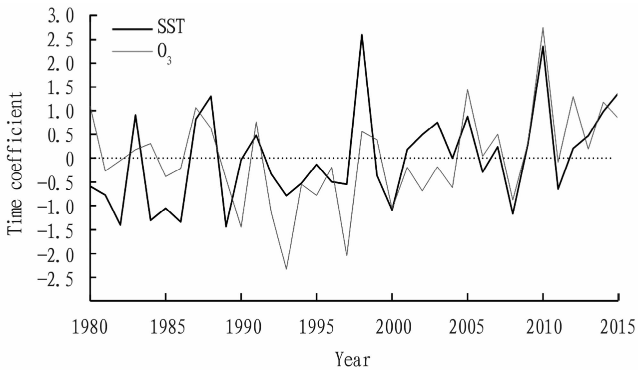

Fig. 6 Time coefficient of the first mode obtained by SVD decomposition for the SST in the tropical Indian Ocean and stratospheric ozone at 70 hPa in East Asia in spring

3.1.2 40 hPa. The correlation coefficient of the first mode obtained by SVD between SST field in the tropical Indian Ocean and the ozone field at 40 hPa in the stratosphere in East Asia in spring was 0.41, and SCF was 72.94%. Similar to 70 hPa, the spring SST in the tropical Indian Ocean also had a good correlation with the stratospheric ozone at 40 hPa in East Asia. As shown in Fig. 9, in the SST field, the whole region presented a consistent positive correlation, and the range of significant correlation areas declined, and the eastern tropical Indian Ocean failed to pass the test. In the ozone field, the correlation coefficient was still negative in the south and positive in the north, but its influence range and region reduced. Similarly, there was a good corresponding relation between the time coefficient of SST and ozone by SVD decomposition (Fig. 8).

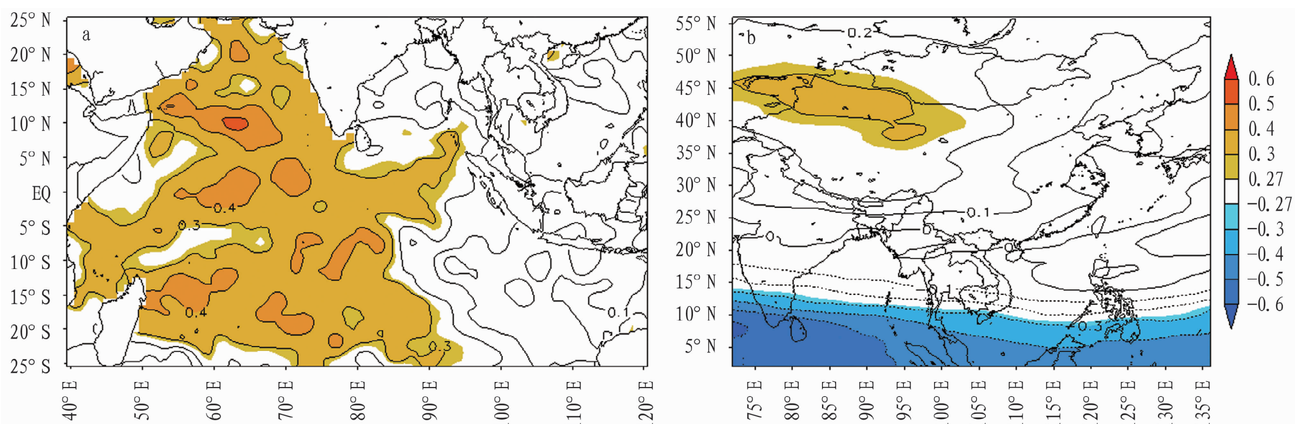

Fig. 7 Spatial distribution of the first mode obtained by SVD decomposition for the SST (a) in the tropical Indian Ocean and stratospheric ozone (b) at 40 hPa in East Asia in spring

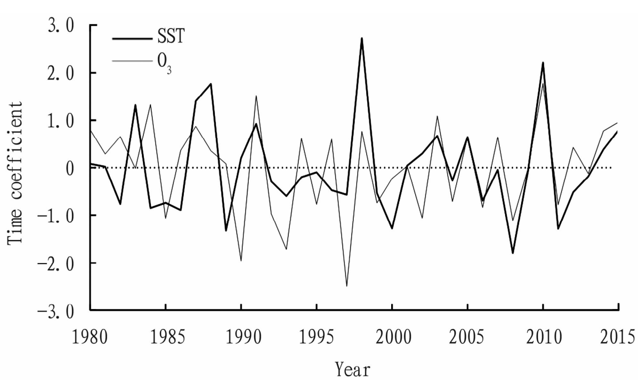

Fig. 8 Time coefficient of the first mode obtained by SVD decomposition for the SST in the tropical Indian Ocean and stratospheric ozone at 40 hPa in East Asia in spring

3.2 Autumn

3.2.1 70 hPa. Fig. 9 shows the spatial distribution of the first mode obtained by SVD decomposition between the SST field in the tropical Indian Ocean and the ozone field at 70 hPa in the stratosphere in East Asia in autumn. The SCF of the first mode was 85.80%, and the correlation coefficient was 0.53. Therefore, the SVD mode corresponding to the first pair of singular vectors can represent the main characteristics of the interaction between the SST field and the ozone field at 70 hPa. As can be seen from Fig. 9, in the SST field, the significant correlation area was large, and the correlation was positive in the west and negative in the east, which was similar to the distribution pattern of positive IOD. However, the significant negative correlation area was small, and was only distributed in the southeast of the tropical Indian Ocean. In the ozone field, there was a positive correlation in the whole region, and the significant correlation areas were distributed in the northeast of China, the area from Lake Balkhash to Lake Baikal, the Bay of Bengal, southeast China and the northwest Pacific Ocean. Compared with the results of correlation analysis at 70 hPa in autumn, there were some differences between them. Firstly, in the SVD decomposition, a significant positive correlation appeared to the north of 45° N in East Asian. Secondly, a significant positive correlation appeared in the region to the south of 15° N where the correlation was not significant in the correlation analysis. The time coefficient of the first mode (Fig. 10) also shows that the correlation between the two had a good corresponding relation in time.

3.2.2 40 hPa. The correlation coefficient of the first mode obtained by SVD between SST field in the tropical Indian Ocean and the ozone field at 40 hPa in the stratosphere in East Asia in autumn was 0.58, and SCF was 82.46%. As shown in Fig. 11, the autumn SST in the tropical Indian Ocean also had a good correlation with the stratospheric ozone at 40 hPa in East Asia. In the SST field, there was a negative correlation in the southeast of the

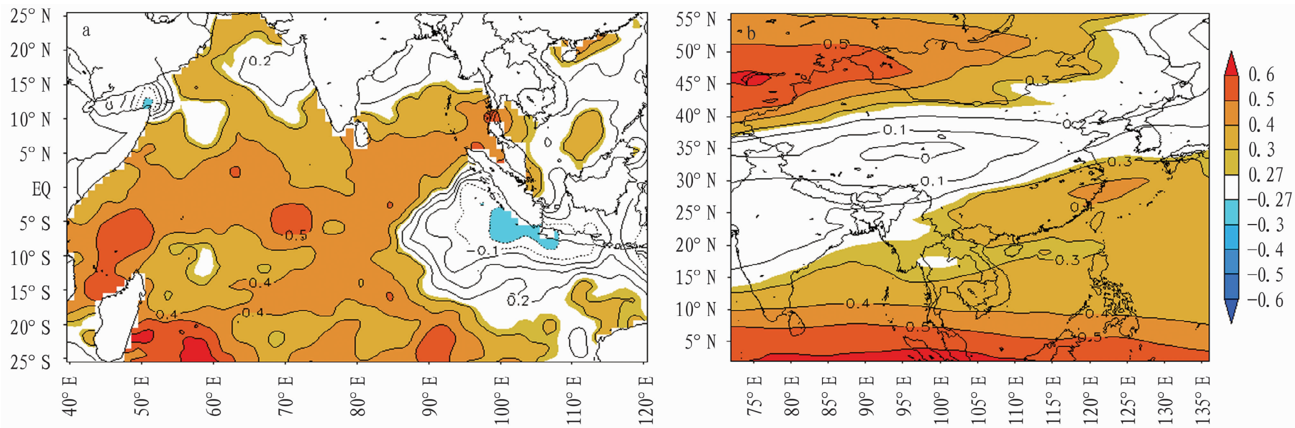

Fig. 9 **Spatial distribution of the first mode obtained by SVD decomposition for the SST (a) in the tropical Indian Ocean and stratospheric ozone (b) at 70 hPa in East Asia in autumn**

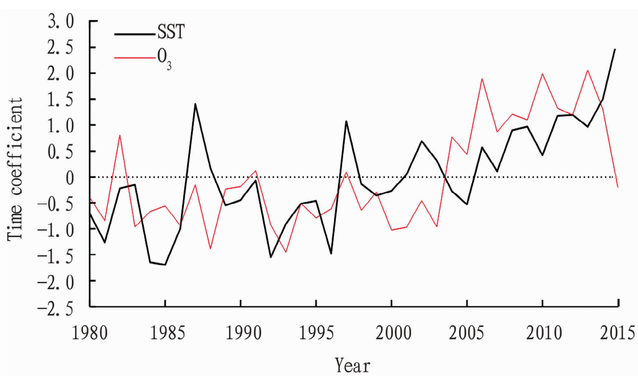

Fig. 10 **Time coefficient of the first mode obtained by SVD decomposition for the SST in the tropical Indian Ocean and stratospheric ozone at 70 hPa in East Asia in autumn**

tropical Indian Ocean, namely the west of Sumatra Island. There was a positive correlation in the center and west of the tropical Indian Ocean, covering almost two-thirds of the ocean surface. In the ozone field, a negative correlation appeared in the middle latitudes of East Asia, and the significant negative correlation areas were located in Inner Mongolia, Lake Baikal and northeast China. The range of positive correlation in the low latitudes extended northward, covering areas to the south of 20° N and southern and eastern China. Compared with the results of SVD decomposition at 70 hPa height in autumn, the positive correlation in the middle latitudes became negative correlation, and the range of the original positive correlation in the low latitudes expanded to the north, while the correlation became strong. Compared with the results of correlation analysis in autumn, there were differences between the two. In the SVD decomposition, there was a significant negative correlation in East Asia.

In the study on the influence of SST changes in the tropical Indian Ocean and ozone layer distribution in East Asia, it is found that there were some differences in the results of correlation analysis and SVD decomposition in autumn, which may be caused by the use of different spatial SST data. That is, the data of IODI used in the correlation analysis were calculated from the difference between regional SST anomalies in the northwest and southeast of the tropical Indian Oceans, while the SST data in the SVD decomposition were SST data for the entire tropical Indian Ocean.

In the SVD analysis of autumn, whether in the lower stratosphere or the upper stratosphere, the correlation near the Tibetan Plateau was always weak, and it was difficult to pass the significance test, which may be caused by the dynamic process resulting from factors such as the high altitude and large terrain of the Tibetan Plateau[21].

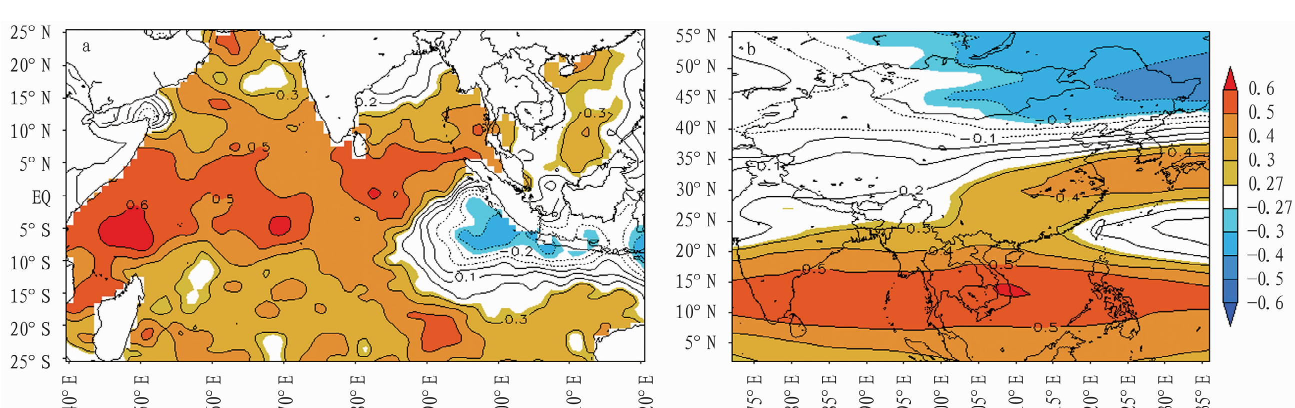

Fig. 11 **Spatial distribution of the first mode obtained by SVD decomposition for the SST (a) in the tropical Indian Ocean and stratospheric ozone (b) at 40 hPa in East Asia in autumn**

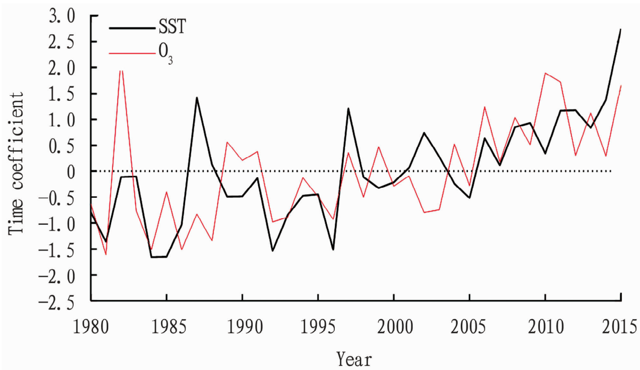

Fig. 12 Time coefficient of the first mode obtained by SVD decomposition for the SST in the tropical Indian Ocean and stratospheric ozone at 40 hPa in East Asia in autumn

From the above analysis, it is found that the changes of SST in the tropical Indian Ocean had a certain impact on ozone in East Asia, and the anomaly of meronal Hadley circulation[22] and the meronal transport of Brewer – Dobson circulation[23] may be one of the physical factors affecting the distribution of ozone layer in East Asia. The role of changes of SST in the tropical Indian Ocean in these meridional circulations and in the physical processes and regulatory mechanisms of ozone layer distribution in East Asia is worthy of further analysis in future studies.

4 Conclusions

On the basis of the study of the two main modes of SST changes in the tropical Indian Ocean, two indexes IOBI and IODI were calculated to characterize IOB and IOD changes during 1980 – 2015. Based on the analysis of correlations between IOBI or IODI and the stratospheric ozone in East Asia, and the SVD decomposition of SST in the tropical Indian Ocean and the stratospheric ozone in East Asia in spring and autumn, the impact of SST changes in the tropical Indian Ocean on the ozone distribution in East Asia and its influencing scope in horizontal and vertical direction were discussed. Some conclusions were obtained as follows.

(1) SST changes in the tropical Indian Ocean had a significant effect on the distribution of stratospheric ozone in East Asia, which changed with seasonal changes and was consistent with the temporal variation of the two main modes of SST changes in the tropical Indian Ocean. It is worth noting that this impact was most significant in spring when IOB was strong and autumn as IOD was strong.

(2) The time series of IOBI and IODI had a good correlation with stratospheric ozone change in East Asia, and it was especially significant in the lower stratosphere (70 hPa) and middle stratosphere (40 hPa). Specifically, IOBI was correlated with stratospheric ozone change negatively in the low latitudes but positively in the middle latitudes in East Asia, and the correlation changed with IOB intensity. IODI was positively correlated with stratospheric ozone change in the middle and low latitudes of East Asia, and the correlation changed with IOD intensity.

(3) According to the SVD decomposition of SST changes in the tropical Indian Ocean and the ozone in East Asia, the effect of spring SST change on the ozone distribution at the isobaric surface of 70 hPa in the middle and low latitudes of East Asia was stronger than that at 40 hPa, which indicated that the effect of IOB on the stratospheric ozone distribution in East Asia mainly appeared in the lower stratosphere. In autumn, the impact of SST changes in the tropical Indian Ocean on stratospheric ozone distribution in East Asia at 40 hPa in the middle latitudes was reverse to that at 70 hPa, meaning that the effect of IOD on ozone distribution gradually weakened with the increase of altitude in the middle latitudes of East Asia.

References

[1] ANGIONE RJ, MEDEIROS EJ, ROOSEN RG. Stratospheric ozone as viewed from the Chappuis band[J]. Nature, 1976, 261(5558): 289.
[2] WANG TJ, SUN ZB. Development of study on ozone variation and its climatic effect[J]. Advance in Earth Science, 1999, 14(1): 37 –43.
[3] GUO SC. Atmospheric ozone variation and its climatic effect[M]. Beijing: China Meteorological Press, 2002.
[4] LIN ZG. The consequences of ozone layer destruction and the countermeasures for its protection[J]. Meteorological Monthly, 1988, 14(11): 52 –53.
[5] NZOTUNGICIMPAYE CM, ABIODUN BJ, STEYN DG. Tropospheric ozone and its regional transport over Cape Town[J]. Atmospheric Environment, 2014, 87(5): 228 –238.
[6] WEN C, HUANG R. The propagation and transport effect of planetary waves in the Northern Hemisphere winter[J]. Advances in Atmospheric Sciences, 2002, 19(6): 1113 –1126.
[7] World Meteorological Organization. Scientific assessment of ozone depletion: 2010, global ozone research and monitoring project-Report No. 52 [R]. 2011.
[8] CHEN W, HUANG RH. The numerical study of seasonal and interannual variabilities of ozone due to planetary wave transport in the middle atmosphere part I: The case of steady mean flows[J]. Chinese Journal of Atmospheric Sciences, 1996, 20(5): 513 –523.
[9] CHEN W, HUANG RH. The numerical study of seasonal and interannual variabilities of ozone due to planetary wave transport in the middle atmosphere part II: The case of steady flow interaction[J]. Chinese Journal of Atmospheric Sciences, 1996, 20(6): 703 –712.
[10] ZHOU BT, WANG HJ. Interannual and interdecadal variations of the Hadley circulation and its connection with tropical sea surface temperature[J]. Chinese Journal of Geophysics, 2006, 49(5): 1271 –1278.
[11] GUO SC, DAI M, YANG PQ, *et al*. Basic state of MMC and its correlation with atmospheric ozone variation[J]. Chinese Journal of Atmospheric Sciences, 2013, 37(1): 36 –42.
[12] GUO SC, HU YY, CHEN CX, *et al*. An analysis on the relationship between atmospheric circulation and the total ozone changes in East Asia [J]. Journal of Yunnan University: Natural Science Edition, 2016, 38 (5): 758 –765.
[13] ZHOU H, JI CP, ZHOU LB, *et al*. ENSO signal in total ozone over Tibet [J]. Climatic and Environmental Research, 2001, 18(3): 267 –272.
[14] HAN Z, ZHOU L, GAO Y, *et al*. Total ozone variation between 50° and 60° N[J]. Geophysical Research Letters, 2005, 32(23): L23812.
[15] RIEDER HE, FROSSARD L, RIBATET M, *et al*. On the relationship between total ozone and atmospheric dynamics and chemistry at mid-latitudes-Part 2: The effects of the El Nino/Southern Oscillation, volcanic eruptions and contributions of atmospheric dynamics and chemistry to long-term total ozone[J]. Atmospheric Chemistry and Physics, 2013, 13(1): 165 –179.
[16] SAJI NH, GOSWAMI BN, VINAYACHANDRAN PN, *et al*. A dipole model in the tropical Indian Ocean[J]. Nature, 1999, 401(6751): 360 –363.
[17] WEBSTER PJ, MOORE AM, LOSCHNIGG JP, *et al*. Coupled ocean-atmosphere dynamics in the Indian Ocean during 1997 – 1998[J]. Nature, 1999, 401(6751): 356 –60.
[18] NASSAR R, LOGAN JA, MEGRETSKAIA IA, *et al*. Analysis of tropical tropospheric ozone, carbon monoxide, and water vapor during the 2006 El-Niño using TES observations and the GEOS-Chem modell[J]. Journal of Geophysical Research Atmospheres, 2009, 114 (D17): D17304.
(To page 15)

(3) In the monthly variation of heat island intensity in Weihai, it reached the highest point (up to 1.64 ℃) in December, gradually decreased to 1.03 ℃ from January to February, rose to 1.46 ℃ from March to May, then continuously decreased to the annual valley value of 0.66 ℃ from August to August, and finally continuously increased to 1.64 ℃ in December. In terms of seasonal variation, urban heat island intensity was the weakest in summer (as low as 0.86 ℃), stronger in spring and autumn (both up to 1.32 ℃), and the strongest in winter (1.38 ℃), which accords with the general law of seasonal variation of urban heat island intensity. This is inconsistent with the seasonal variation of urban heat island intensity in southern China, which may be related to central heating in winter in northern China.

(4) Seen from the diurnal, monthly, seasonal and annual variations of urban heat island intensity in Weihai, it was the strongest when temperature was the lowest, and the weakest when temperature was the highest, showing an obvious "inverse phase" with the temperature change. This is due to the "thermal hysteresis effect" caused by the significantly higher thermal conductivity and heat capacity of the underlying surface in the urban areas than that in the suburban areas.

(5) The high-value area of urban heat island intensity in Weihai was highly consistent with human residential activity areas and industrial and commercial intensive areas, and the extension trend of heat island intensity was also the same as the direction of urban development and construction. The "cold island phenomenon" in some offshore areas may be related to the geographical location, terrain and the southeast monsoon in summer.

(6) Based on the specific geological landform, water network and limited water and soil resources of Weihai City, urban heat island effect can be alleviated by optimizing the types and distribution of vegetation communities, rationally planning and constructing urban water bodies, promoting green building materials and adjusting the shape design.

The optimized weather station data method was used to analyze the spatial and temporal variation characteristics of heat island effect in Weihai City, and the length of data series and the number of observation stations were taken into account. The quantitative results are intuitive, and the evaluation conclusions are objective, which are easy to be accepted by the public and decision-making services. However, it is still necessary to strengthen research on the fine distinction between urban and suburban weather stations, quality control and screening of data, how to integrate weather station data method, remote sensing inversion and numerical simulation, and how to carry out multi-dimensional and deep comprehensive expansion and extension from unilateral study of urban heat island effect to urban thermal environment, heat island circulation and heat island formation mechanism.

References

[1] YANG YH, XU XD, WENG YH. Simulation of daily cycle of boundary layer heat island in Beijing[J]. Quarterly Journal of Applied Meteorology, 2003(1): 61-68.

[2] KARL TR, DIAZ HF, KUKLA G. Urbanization: Its detection and effect in the United States climate record[J]. Journal of Climate, 1988(1): 1099-1123.

[3] KUKLA G, GAVIN J. Urban warming[J]. Journal of Climate and Applied Meteorology, 1986(25): 1265-1270.

[4] ZHOU SZ, ZHANG C. Urban heat island effect in Shanghai[J]. Acta Geographica Sinica, 1982(4): 372-382.

[5] STEWARI ID, OKE TR. Local climate zones for urban temperature studies[J]. Bulletin of the American Meteorological Society, 2012, 93(12): 1879-1900.

[6] LIU WD, YANG P, YOU HL, *et al.* Heat island effect and diurnal range in Beijing [J]. Climatic and Environmental Research, 2013, 18(2): 171-177.

[7] MAO CZ, Zhang M, Liu YP, *et al.* Analysis of urban heat island in Yichang based on automatic weather station data[J]. Journal of Desert & Oasis Meteorology, 2019, 15(1): 103-110.

[8] WALIJIANG WHT, REN GY, SUN XB. The daily temperature characteristics of the intensity of urban heat island in Urumqi and seasonal changes [J]. Desert and Oasis Meteorology, 2018, 12(1): 21-28.

[9] SHANG JS, LI BL, SUN XL, *et al.* Characteristic analysis of urban heat island effect in summer in Ji'nan City[J]. Journal of Arid Meteorology, 2018, 36(1): 70-74.

[10] LONG S, SU X, WANG YN, *et al.* Research progress in cooling and humidifying efficiency of urban green spaces[J]. Forest Engineering, 2016, 32(1): 21-24.

[11] YU ZW, GUO QH, SUN RH. Impacts of urban cooling effect based on landscape scale: A review[J]. Chinese Journal of Applied Ecology, 2015, 26(2): 636-642.

[12] PENG J, LIU Q, XU Z, *et al.* How to effectively mitigate urban heat island effect? A perspective of waterbody patch size threshold[J]. Landscape and Urban Planning, 2020, 202: 103873.

[13] SUN R, CHEN L. How can urban water bodies be designed for climate adaptation[J]. Landscape and Urban Planning, 2012, 105(1-2): 27-33.

[14] TAN X, SUN X, HUANG C, *et al.* Comparison of cooling effect between green space and water body[J]. Sustainable Cities and Society, 2021, 67: 102711.

[15] SUN R, CHEN A, CHEN L, *et al.* Cooling effects of wetlands in an urban region: The case of Beijing[J]. Ecological Indicators, 2012, 20: 57-64.

[16] HONG J, TENG S, ZHANG R. Effect of water body forms on microclimate of residential district[J]. Energy Procedia, 2017, 134: 256-65.

(From page 7)

[19] TAKASHI S, KENGO S. Role of meteorological variability in global tropospheric ozone during 1970 - 2008[J]. Journal of Geophysical Research, 2012, 117(117): 18303.

[20] KRZYSCIN JW. El Niño-Southern Oscillation and Indian Ocean Dipole contribution to the zonal mean total ozone in the Northern Hemisphere[J]. International Journal of Climatology, 2016: 37(8): 3517-3524.

[21] ZHOU XJ, LUO C, LI WL, *et al.* Change of total ozone in China and the low value center of Qinghai-Tibet Plateau[J]. Chinese Science Bulletin, 1995, 40(15): 1396-1398.

[22] GUO SC, LI Q, LIU Y, *et al.* Characteristics of local Hadley circulation and its relation to atmospheric ozone over the low-latitude regions in East Asia[J]. Journal of Tropical Meteorology, 2012, 28(4): 478-486.

[23] CHEN QL, CHEN YJ. Stratospheric residual circulation and its temporal and spatial evolution[J]. Chinese Journal of Atmospheric Sciences, 2007, 31(1): 137-144.